JACS
JOURNAL OF THE AMERICAN CHEMICAL SOCIETY
Article
pubs.acs.org/JACS

Mechanistic Rationalization of Unusual Sigmoidal Kinetic Profiles in the Machetti–De Sarlo Cycloaddition Reaction

Matthew P. Mower and Donna G. Blackmond*

Department of Chemistry, The Scripps Research Institute, La Jolla, California 92037, United States

Supporting Information

ABSTRACT: Unusual sigmoidal kinetic profiles in the Machetti–De Sarlo base-catalyzed 1,3-dipolar cycloaddition of acrylamide to *N*-methylnitroacetamide are rationalized by detailed in situ kinetic analysis. A dual role is uncovered in which a substrate acts as a precursor to catalyze its own reaction. Such kinetic studies provide a general protocol for distinguishing among different mechanistic origins of induction periods in complex organic reactions.

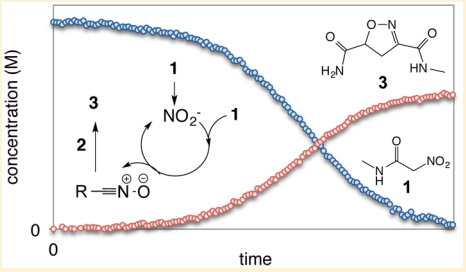

INTRODUCTION

Temporal kinetic profiles of complex multistep organic reactions provide a wealth of mechanistic information that, when deconvoluted, may help to support or refute a proposed reaction mechanism as well as to suggest other experiments to test the mechanism further.[1] Kinetic profiling can be especially useful in cases where detection of intermediates may be difficult, such as in the case of Jacobsen's enantioselective amido-thiourea-catalyzed hydrocyanation of imines, in which reaction progress kinetic analysis and DFT transition-state calculations supported a mechanism based on non-covalent catalyst–substrate interactions rather than direct activation of the substrate via strong catalyst binding.[2] Reactions that exhibit saturation kinetics,[3] catalyst activation/deactivation,[4] product acceleration/inhibition,[5] or nonlinear effects of catalyst enantiopurity[6] represent other examples where monitoring the temporal kinetic profile has been shown to be a valuable mechanistic tool.

Reactions exhibiting sigmoidal kinetic profiles provide a key case where kinetic analysis can provide mechanistic clues. Sigmoidal profiles complicate attempts to obtain kinetic data via conventional initial rate measurements, and in situ observation of reaction progress can prove essential in such cases, as examples demonstrate. Non-enzymatic self-replicating systems based on template-directed autocatalysis studied in the context of the origin of life on prebiotic earth have been demonstrated to show sigmoidal growth profiles.[7] Sigmoidal profiles are also a characteristic of the exponential amplification of polymerase chain reaction (PCR)-based methods in biochemistry,[8] and other supramolecular catalytic systems have been likened to such amplification processes on the basis of the similarity of their kinetic profiles.[9] Exhaustive mechanistic detail has been extracted from kinetic profiles of the asymmetric autocatalytic alkylation of pyrimidyl aldehydes (Soai reaction[10]), which exhibits the sigmoidal profile characteristic of a self-replication process.[11] The Finke–Watkzy mechanism, originally developed for nucleation and growth of transition metal nanoclusters,[12] exquisitely rationalizes sigmoidal kinetic profiles in a wide range of phenomena,[13] including neurological protein aggregation.[14]

RESULTS AND DISCUSSION

Figure 1 illustrates a number of experimental examples from our laboratories of reactions bearing the signature of a sigmoidal kinetic profile, compared to that of conventional first-order kinetics. Catalyst activation in Heck coupling reactions under dry conditions using Pfaltz's C,N-palladacycle ligands led to slow introduction of the active Pd species to the cycle[4a] (Figure 1, blue). As already mentioned, the Soai autocatalytic reaction is a singular example of small-molecule

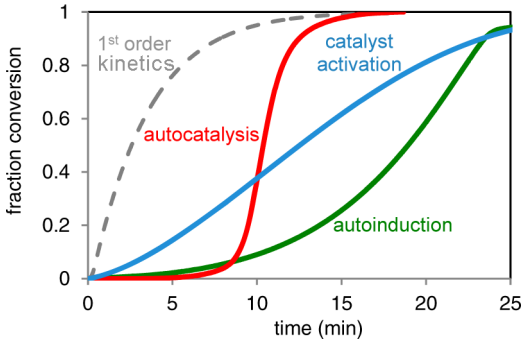

Figure 1. Experimental kinetic profiles comparing conventional first-order kinetics (gray) to distinct examples of sigmoidal kinetics: red, the autocatalytic Soai reaction;[10] blue, catalyst activation in Heck reactions using a C,N-palladacycle precatalyst;[5] green, autoinduction in the proline-catalyzed aminoxylation of propionaldehyde.[5a]

Received: December 15, 2014
Published: January 22, 2015

DOI: 10.1021/ja512753v
J. Am. Chem. Soc. 2015, 137, 2386–2391

self-replication[11] (Figure 1, red). A more common observation is the case where the reaction product or a byproduct accelerates the reaction rate but cannot replicate itself in the absence of another catalyst;[5a] such behavior is differentiated from true self-replication by the term "autoinduction" (Figure 1, green).[15] The unusual kinetics illustrated in the examples of Figure 1 occur for fundamentally different underlying mechanistic reasons. Uncovering the origin of the unusual kinetic profile is key to interpreting the mechanism of the reaction in each case.

We report here detailed kinetic and mechanistic studies uncovering the origin of unusual sigmoidal kinetic behavior reported by De Sarlo, Machetti, and co-workers[16] in base-catalyzed cycloaddition/condensation of nitro compounds in water (Scheme 1). These reactions provide convenient access

Scheme 1. Machetti–De Sarlo Cycloaddition

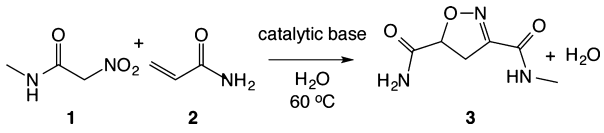

to isooxazoles or 2-isooxazolines, which can lead to stereoselective synthesis of γ-amino alcohols and β-hydroxy ketones. The reaction has most recently been used to prepare functionalized fullerenes.[16f] Sigmoidal kinetic profiles were observed in the reaction carried out in both organic solvents and water, behavior that was suggested as being related to multistep reaction pathways. Our studies help to provide mechanistic understanding through a detailed probe of the kinetic behavior of this reaction, highlighting an unusual case where a molecule acts both as a substrate and as a precursor to a catalyst in its own transformation. In addition, this example allows development of a general protocol for distinguishing among possible origins of sigmoidal kinetic profiles.

Figure 2 shows a temporal profile of the reaction of Scheme 1 monitored by FTIR spectroscopy. Concentration measured

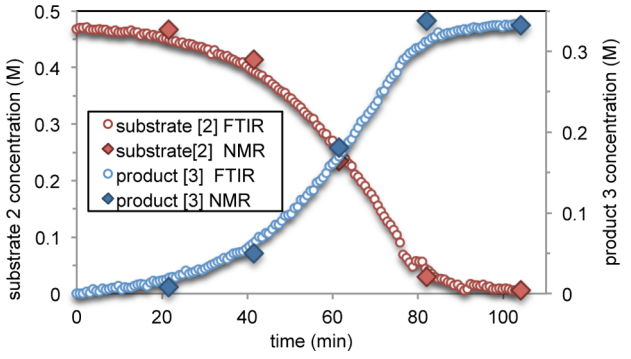

Figure 2. Temporal kinetic profile of substrate **2** and product **3** in the reaction of Scheme 1 carried out with 10 mol% NaOH as base. $[\mathbf{1}]_0$ = 0.45 M; $[\mathbf{2}]_0$ = 0.33 M; 60 °C.

by quantitative NMR spectroscopy from aliquots taken periodically over the course of the reaction serves to validate the in situ measurement. The sigmoidal kinetics in product formation observed by De Sarlo, Machetti, and co-workers are reproduced here. Interestingly, these data reveal that the substrate and product kinetic profiles are approximately symmetric in shape.

As noted above, sigmoidal kinetic profiles may arise for a number of distinct reasons. One of the simplest cases, invoked in this case[16] and often cited for chain reactions due to the non-steady-state buildup of intermediate species,[17] is that of a sequential reaction series where intermediate species such as **B** and **C** form from a reactant **A**, building up to steady-state concentrations and reacting further to give product **D** (eq 1).

$$\mathbf{A} \underset{k_{-1}}{\overset{k_1}{\rightleftarrows}} \mathbf{B} \underset{k_{-2}}{\overset{k_2}{\rightleftarrows}} \mathbf{C} \xrightarrow{k_3} \mathbf{D} \qquad (1)$$

While such a multistep sequence can yield kinetic profiles exhibiting an induction period in product formation, as shown in Figure 3, it is critical to note that sigmoidal product profiles

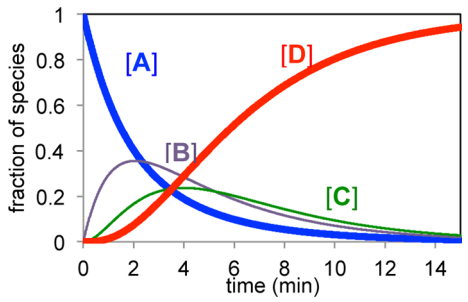

Figure 3. Kinetic profiles simulated for species **A**, **B**, and **C** in the consecutive multistep reaction of eq 1. $[\mathbf{A}]_0$ = 1 M; $k_1 = k_2 = k_3$ = 0.5 s^{-1}; $k_{-1} = k_{-2}$ = 0.1 s^{-1}.

occur necessarily at the expense of reactant concentration in the non-steady-state buildup of stoichiometric quantities of intermediates. Other kinetic scenarios, such as higher order kinetics in the buildup and consumption of intermediates,[17] may result in extended induction periods for product formation, but again at the expense of substrate concentration. Hence, observation of symmetry between substrate and product kinetic traces, as in Figure 2, is sufficient to confirm that a sequence of consecutive reactions with intermediate buildup cannot rationalize the behavior observed for the cycloaddition reaction shown in Scheme 1. Instead, the data of Figure 2 suggest a mechanism that permits slow in situ formation of *catalytic* quantities of a key intermediate.

Another common explanation for sigmoidal kinetic profiles is the case where the product of the reaction accelerates its rate or acts as a catalyst in its own formation. A simple way to probe this hypothesis is to monitor reaction rate with product added to the reaction mixture. Figure 4 compares profiles of the reaction of Scheme 1 carried out with and without addition of product **3**, showing that the reaction product may serve to shorten slightly but not eliminate the induction period. Variation was observed in the length of the induction period, even for reactions carried out under identical conditions but without product added (see Supporting Information), making the difference in induction time for the two runs in Figure 4 difficult to interpret. As has been noted before, variation in induction behavior observed in both chemical[11c] and physical[18] processes implies that some type of stochastic events occur to produce the conditions for reaction light-off. In addition, in the present case, the subsequent reaction rates following the induction period are similar in the presence and absence of product, as can be seen by the overlay of the two curves of Figure 4 shifted in time. This result suggests that neither true

DOI: 10.1021/ja512753v
J. Am. Chem. Soc. 2015, 137, 2386–2391

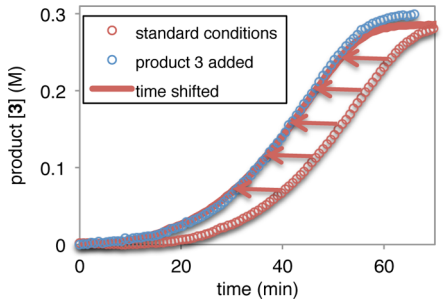

Figure 4. Experimental kinetic profiles for the reaction of Scheme 1 carried out in the presence and absence of added reaction product **3**. $[\mathbf{1}]_0$ = 0.45 M; $[\mathbf{1}]_0$ = 0.30 M; base = NaOH = 0.03 M. Open red circles, no product **3** added; open blue circles, 0.30 M product **3** added (added product subtracted from product formed during the reaction); red line, standard conditions curve shifted in time by 10 min as indicated by arrows.

autocatalysis nor product acceleration can account for the unusual kinetic behavior.

Changes in acidity/basicity of the reaction mixture can provide another rationale for unusual temporal profiles. The influence of the acidity of the medium on the induction period investigated by in situ monitoring of reaction pH showed that the reaction mixture became slightly more acidic over the course of the reaction (Figure 5). The role of pH in the

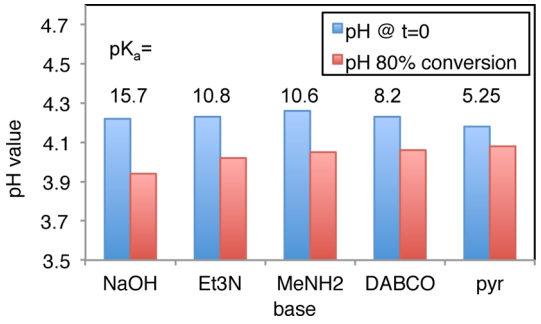

Figure 5. Variation of pH between reaction outset and the end of the sigmoidal curve (ca. 80% conversion) for the reaction of Scheme 1 carried out with different bases. $[\mathbf{1}]_0$ = 0.45 M; $[\mathbf{2}]_0$ = 0.30 M; [base] = 0.03 M.

induction behavior is not simple to deconvolute: at higher base concentration, the final pH value was found to be higher than the initial value for reactions at lower base concentration (see Supporting Information), even while similar induction periods were observed. The reaction proceeds with similar sigmoidal behavior using a variety of organic bases of differing strength as well as with NaOH, and the length of the induction period shows no correlation with base pK_a.

When the reaction is carried out at the same base concentration with bases differing in pK_a by 10 logs, a similar initial pH value and a similar overall decrease in pH are observed over the course of the reaction for all bases (Figure 5). Buffering the reaction solution resulted in suppression of activity. Thus, neither the absolute value of pH nor the strength of the catalytic base correlates with the induction behavior.

In the absence of the acrylamide reaction partner **2** but in the presence of catalytic base, nitroacetamide **1** concentration was observed to decay slowly over time. Interestingly, we found that if the acrylamide **2** is not introduced to the reaction mixture until *after* a short initial period of substrate **1** decay, the induction period is eliminated, and the reaction immediately exhibits overall zero-order kinetics in both substrates [**1**] and [**2**], as illustrated in Figure 6 for DABCO as base. Reaction rate in the zero-order regime following delayed addition of **2** is proportional to the catalytic concentration of base employed.

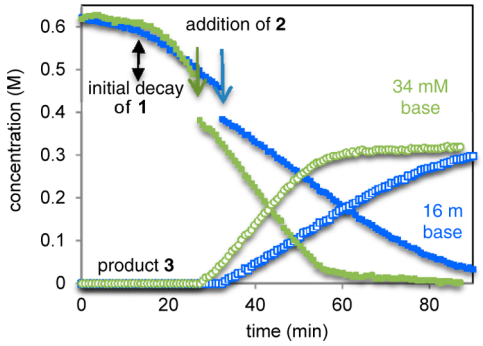

Figure 6. Kinetic profiles for substrate **1** (closed symbols) and product **3** (open symbols) for the reaction of Scheme 1 carried out by addition of **2** following initial partial decomposition of **1**. $[\mathbf{1}]_0$ = 0.62 M; $[\mathbf{3}]_0$ = 0.30 M; [DABCO] = 34 mM (green) or 16 mM (blue).

Identical zero-order rates are observed in the cycloaddition reaction upon addition of **2** for different amounts of pre-decomposition of **1** in excess of the amount of employed base, as shown in Figure 7 for NaOH as base. Similar behavior was

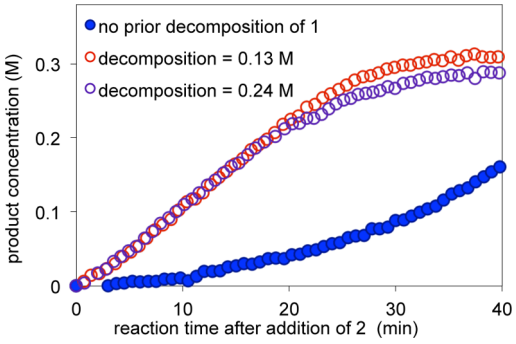

Figure 7. Kinetic profiles of product in the reaction of Scheme 1 carried out by addition of **2** following partial decomposition of **1** to the amounts shown. $[\mathbf{1}]_0$ = 0.6 M; $[\mathbf{3}]_0$ = 0.3 M; [NaOH] = 0.03 M. Reaction time is measured from the point of addition of substrate **2** after the indicated in situ pre-decomposition of **1**. Standard reaction (no prior decomposition of **1**) includes **2** from the outset.

observed for the other bases under study (see Supporting Information). Thus, the decomposition of **1** results in the production of a catalytic species that forms in direct proportion to the concentration of base employed, and this species catalyzes the cycloaddition reaction.

The data in Figures 6 and 7 serve to deconvolute the intrinsic kinetic dependences of the Machetti–De Sarlo reaction of Scheme 1 from the processes that take place during the induction period. The intrinsic concentration dependences of the reaction of Scheme 1 show zero-order kinetics in the concentrations of both substrates **1** and **2** and first-order kinetics in the concentration of added base. Importantly, these data reveal that the intrinsic reaction rate does *not* increase with time, further ruling out the case for a truly autocatalytic reaction (Figure 2).

DOI: 10.1021/ja512753v
J. Am. Chem. Soc. 2015, 137, 2386–2391

Decomposition of nitro compounds under a variety of conditions has been reported.[19] Suggested pathways for the decomposition of substrate **1** and the identity of the species formed in the presence of base are postulated in Scheme 2.

Scheme 2. Proposed Reactions of Substrate 1

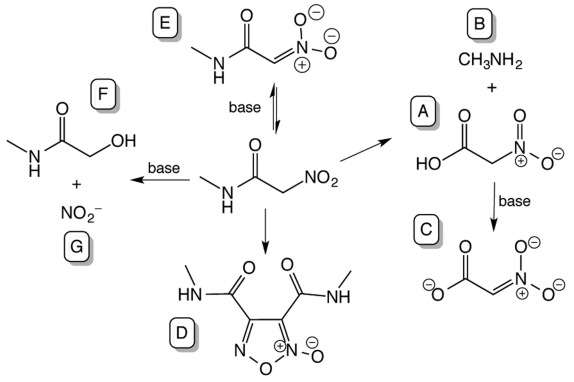

Species **D** was observed and isolated from decomposition of substrate **1** in the absence of substrate **2** and has been reported previously by spectroscopic identification and by isolation.[16c] The nitronate species **E** was observed to form immediately and quantitatively from the base at the beginning of all reactions; however, species **E** is ruled out as an active substrate, as no conversion is observed when a full equivalent of **E** is employed in the reaction instead of substrate **1**. Other species in Scheme 2 were not directly observed during in situ monitoring of the reaction.

The potential role of such decomposition products in the autoinduction process may be probed by observing the effect on the induction period of adding the various proposed decomposition products to the reaction mixture. Figure 8

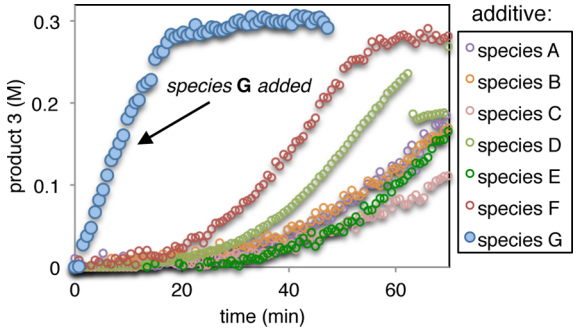

Figure 8. Kinetic profiles of product in the reaction of Scheme 1 carried out with 0.025–0.03 M additives **A**–**G** as designated in Scheme 2. $[\mathbf{1}]_0$ = 0.45 M; $[\mathbf{2}]_0$ = 0.30 M; [NaOH] = 0.03 M; 60 °C.

shows that none of the species shown in Scheme 2 resulted in elimination of the induction period when added to the reaction except NO_2^- (similar results were found with counterions Na^+, K^+, or Bu_4N^+, see Supporting Information). This implies a role for NO_2^- in an autoinductive process.

Induction periods may be observed when a side product formed from a separate reaction of a substrate can act as a catalyst for the primary reaction of that substrate. Autoinductive behavior is then a consequence of higher order kinetics arising from involvement of two substrate molecules in a single elementary reaction step—one directly as a reactant and one as a catalyst indirectly derived from the substrate—giving overall second-order kinetics in [substrate]. For example, in studies of prebiotically plausible hydration reactions of α-aminonitriles, Commeyras and co-workers[20] suggested that the reaction is catalyzed by aldehydes that are themselves formed from partial decomposition of the substrate aminonitrile. This feedback loop between a substrate and its reaction product provides a form of rate amplification. While such an autoinductive effect is clearly distinct from the prebiotic implications of true self-replication, autoinductive processes have relevance in models for prebiotic metabolism because they develop reactants and catalysts from the same building blocks.

Rationalizing the autoinductive effect of nitrite ion **G** in the reaction of Scheme 1 requires consideration of mechanisms that have been proposed for the reaction, as shown in Scheme 3. One main question hinges on whether dehydration occurs

Scheme 3. Proposed Reaction Pathways

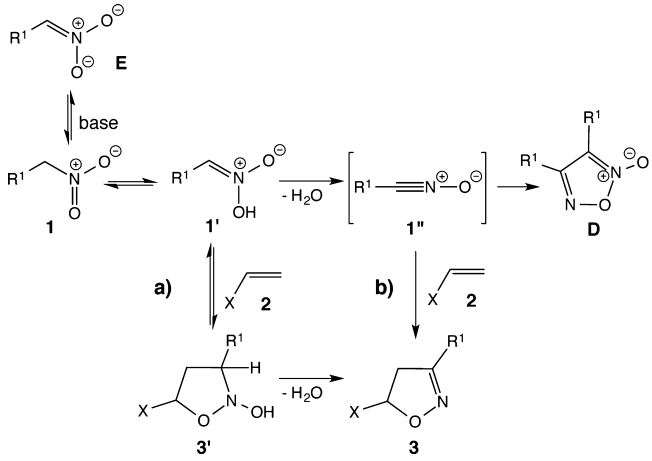

before or after the cycloaddition step. De Sarlo, Machetti, and co-workers favor pathway a—the cycloaddition of **2** to **1′**, the tautomer of **1**, occurring prior to dehydration—for reactions in water, and pathway b—a route via the nitrile oxide—for reactions in chloroform. As noted earlier, however, neither of these pathways as simply written can rationalize an induction period that is symmetric in product formation *and* substrate consumption.

A significant role for route b in Scheme 3 with a nitrile oxide intermediate was discounted by De Sarlo and Machetti for reactions in water because the nitro substrate was found to be essentially unreactive in the absence of the dipolarophile if base was not present, while the cycloaddition reaction itself may proceed slowly even in the absence of added base. For example, complete conversion to the cycloaddition product between **1** and acrylamide **2** was observed, accompanied by a significant induction period, within 24 h in the absence of base, while in the absence of both **2** and base, only minimal decomposition of **1** occurred over the same time period. The lack of observable decomposition of **1** was suggested to imply that no nitrile oxide was formed. However, we confirmed the presence of nitrite ion **G** by the Griess colorimetric test even before significant decomposition of **1** was detected (see Supporting Information), implying that a route to catalytic quantities of the nitrile oxide could be present even in the absence of significant substrate decomposition. The sigmoidal kinetic profile observed by De Sarlo and Machetti in the cycloaddition reaction in the absence of base[16d] is consistent with the extremely slow decomposition of **1** to form a catalytic intermediate, unassisted by added base.

DOI: 10.1021/ja512753v
J. Am. Chem. Soc. 2015, 137, 2386–2391

Thus, the same mechanism applies once nitrite ion is present in the system.

Reactions of nitrite ions with nitro compounds, including the formation of nitrile oxide, have been described.[21] The role of nitrite ion in the formation of nitrile oxide may be envisioned in two ways, as shown in Scheme 4. Species **G** may serve as a

Scheme 4. Proposed Roles for Nitrite Ion in Formation of Nitrile Oxide

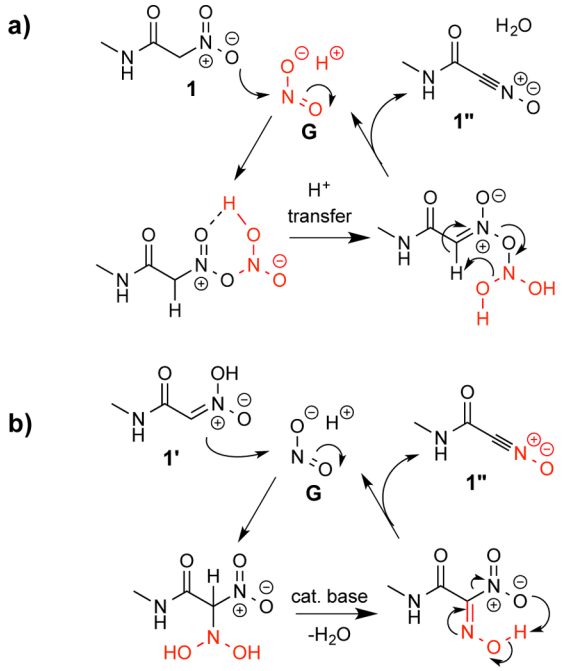

catalytic intermediate analogous to nitrile oxide formation via the dehydration of isocyanates,[22] as illustrated in Scheme 4a, or it may itself become incorporated into the nitrile oxide, with **G** being regenerated from the nitro group of substrate **1**, as shown in Scheme 4b. Reactions carried out using ^{15}N-labeled nitrite show incorporation of the labeled nitrogen into the cycloaddition product, suggesting that the route in Scheme 4b is at least partially operative (see Supporting Information).

Indeed, pathway b via the nitrile oxide coupled with its autoinductive formation as shown in Scheme 4 can rationalize the observed induction period for reactions both in the presence and in the absence of base. These schemes are also consistent with the zero-order intrinsic kinetic dependences of rate on both substrates **1** and **2**, as well as, in the case of reactions with base, the first-order dependence on base. The dual role of **1** in supplying the catalyst and acting as substrate rationalizes the sigmoidal kinetic behavior and is highlighted in red in Scheme 5. Kinetic modeling of the elementary steps as shown in Scheme 5 gave an excellent fit to the experimental data both for the standard conditions and for reactions with added NO_2^- (species **G**), as shown in Figure 9 (see Supporting Information), providing further support to the mechanistic proposal.

Figure 10 illustrates the kinetic profiles of the catalytic intermediates shown in Scheme 5 over the course of the reaction under standard conditions, as revealed in the kinetic model of Figure 8. At the outset of the reaction, the added base is sequestered quantitatively as **E**, the nitronate salt of **1**, in a reaction whose equilibrium lies far toward **E**. Thus, the base is

Scheme 5. Proposed Catalytic Cycle for the Reaction of Scheme 1

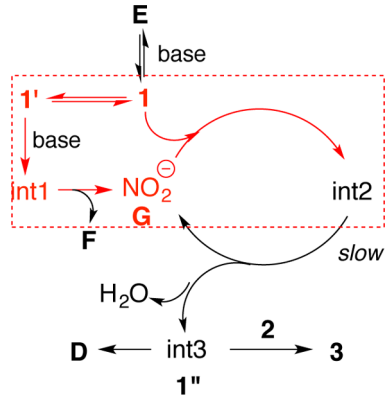

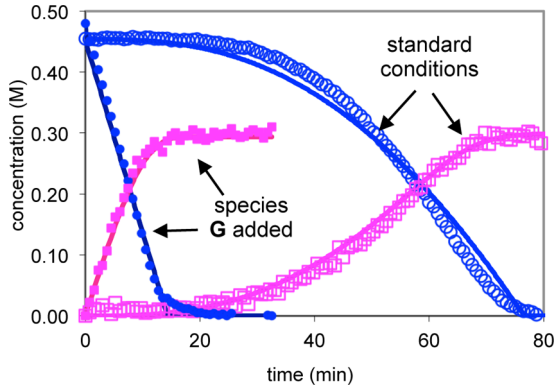

Figure 9. Experimental kinetic profile of the reaction of Scheme 1 from Figure 1 (symbols) compared with the profile for the kinetic model shown in Scheme 5 (lines). Circles, substrate **1**; squares, product **3**; open symbols, standard reaction conditions exhibiting induction period; filled symbols, reaction with species **G** ($NaNO_2$) added at the outset of the reaction.

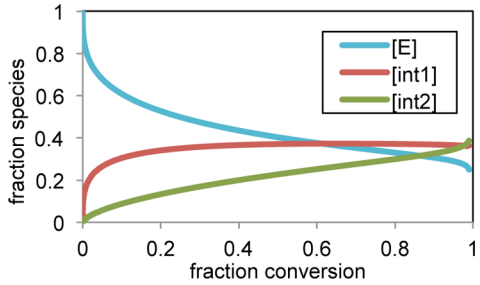

Figure 10. Simulated kinetic profiles of the main catalytic intermediates in the network of Scheme 5 from the kinetic model results of Figure 9.

drawn out of this equilibrium to induce the decomposition of **1** via **int1** to form NO_2^-. The quantity of **1** that can readily decompose to form NO_2^- (irreversibly via **int1**) is limited to the amount of base present. The cycle then proceeds with nitrite ion **G** as catalyst under steady-state kinetics, which includes the reaction of **1** with **G** to form **int2**, the resting state of the catalytic cycle. This species slowly dehydrates to form the nitrile oxide **int3** (**1**′′) in the rate-determining step, followed by fast cycloaddition of **2** to form product **3**, and regenerate NO_2^-, completing the catalytic cycle. The concentrations of **1**′, **G**, and **int3** remain fleeting throughout the reaction, except in the case

DOI: 10.1021/ja512753v
J. Am. Chem. Soc. 2015, 137, 2386−2391

where **G** is added at the outset. Saturation in [**int2**] within the cycle itself rationalizes zero-order kinetics in [**1**]; zero-order kinetics in [**2**] is observed because **2** enters the cycle after rate-limiting formation of **int3**.

CONCLUSION

The unusual sigmoidal kinetic profile in the 1,3-dipolar cycloaddition/condensation of nitro compounds first observed by De Sarlo and Machetti is rationalized on the basis of detailed kinetic analysis. The observation of near symmetry between the sigmoidal substrate decay and product appearance curves precludes an explanation based on the transient features of a simple multistep stoichiometric reaction sequence. When the autoinductive behavior is deconvoluted from the intrinsic kinetics of the catalytic cycle, the distinct signature of the sigmoidal reaction progress curves may be distinguished from similar kinetic behavior with different mechanistic origins, including true self-replicative autocatalysis, simple catalyst activation, and product acceleration. In this case the sigmoidal behavior is attributed to the dual role of nitroacetamide substrate **1** as both a substrate and a catalyst precursor in its own reaction. The use of reaction profiling is key to distinguishing such kinetic features, which may lie behind other seemingly simple transformations. Differentiating between the different origins of unusual kinetic behavior is critical to its potential exploitation in reaction development and optimization as well as for addressing fundamental mechanistic questions including those related to kinetic models for prebiotic metabolism.

ASSOCIATED CONTENT

Supporting Information

Experimental details, crystal structure information, and NMR spectra. This material is available free of charge via the Internet at http://pubs.acs.org.

AUTHOR INFORMATION

Corresponding Author

*blackmond@scripps.edu

Notes

The authors declare no competing financial interest.

ACKNOWLEDGMENTS

Funding from NSF International Collaboration in Chemistry (CHE-1128395) and the Simons Foundation Collaboration on the Origins of Life (SCOL award no. 287625) are gratefully acknowledged. The authors thank Dr. Ryan Shenvi for fruitful discussions.

REFERENCES

(1) (a) Blackmond, D. G. *Angew. Chem., Int. Ed.* **2005**, *44*, 4302. (b) Mathew, J. S.; Klussmann, M.; Iwamura, H.; Valera, F.; Futran, A.; Emanuelsson, E. A. C.; Blackmond, D. G. *J. Org. Chem.* **2006**, *71*, 4711.

(2) Zuend, S. F.; Jacobsen, E. N. *J. Am. Chem. Soc.* **2009**, *131*, 15359.

(3) Rosner, T.; Le Bars, J.; Pfaltz, A.; Blackmond, D. G. *J. Am. Chem. Soc.* **2001**, *123*, 1848.

(4) (a) Rosner, T.; Pfaltz, A.; Blackmond, D. G. *J. Am. Chem. Soc.* **2001**, *123*, 4621. (b) Shekhar, S.; Ryberg, P.; Hartwig, J. F.; Mathew, J. S.; Blackmond, D. G.; Strieter, E. R.; Buchwald, S. L. *J. Am. Chem. Soc.* **2006**, *128*, 3584−3591. (c) Blackmond, D. G.; Schultz, T.; Mathew, J. S.; Loew, C.; Rosner, T.; Pfaltz, A. *Synlett* **2006**, *18*, 3135.

(5) (a) Mathew, S. P.; Klussmann, M.; Iwamura, H.; Wells, D. H., Jr.; Armstrong, A.; Blackmond, D. G. *Chem. Commun.* **2006**, 4291. (b) Phua, P. H.; Mathew, S. P.; White, A. J. P.; de Vries, J. G.; Blackmond, D. G.; Hii, K. K. *Chem.—Eur. J.* **2007**, *13*, 4602.

(6) (a) Blackmond, D. G. *J. Am. Chem. Soc.* **1997**, *119*, 12934. (b) Blackmond, D. G. *Acc. Chem. Res.* **2000**, *33*, 402.

(7) (a) von Kiedrowski, G. *Angew. Chem., Int. Ed. Engl.* **1986**, *25*, 932−935. (b) Chen, J.; Körner, S.; Craig, S. L.; Lin, S.; Rudkevich, D. M.; Rebek, J., Jr. *Proc. Natl. Acad. Sci., U.S.A.* **2002**, *99*, 2593−2596. (c) Sadownik, J. W.; Philp, D. *Angew. Chem., Int. Ed.* **2008**, *51*, 9965−9970.

(8) (a) Blow, N. *Nat. Methods* **2007**, *4*, 869−875. (b) Saiki, R. K.; Bugawan, T. L.; Horn, G. T.; Mullis, K. B.; Erlich, H. A. *Nature* **1986**, *324*, 163−166.

(9) Yoon, H. J.; Mirkin, C. A. *J. Am. Chem. Soc.* **2008**, *130*, 11590−11591.

(10) (a) Soai, K.; Shibata, T.; Morioka, H.; Choji, K. *Nature* **1995**, *378*, 767. (b) Kawasaki, T.; Matsumura, Y.; Tsutsumi, T.; Suzuki, K.; Ito, M.; Soai, K. *Science* **2009**, *324*, 492. (c) Soai, K.; Kawasaki, T. *Chem. Today* **2009**, *27*, 3.

(11) (a) Blackmond, D. G.; McMillan, C. R.; Ramdeehul, S.; Schorm, A.; Brown, J. M. *J. Am. Chem. Soc.* **2001**, *123*, 10103. (b) Buono, F. G.; Blackmond, D. G. *J. Am. Chem. Soc.* **2003**, *125*, 8978. (c) Quaranta, M.; Gehring, T.; Odell, B.; Brown, J. M.; Blackmond, D. G. *J. Am. Chem. Soc.* **2010**, *132*, 15104.

(12) (a) Watzky, M. A.; Finke, R. G. *J. Am. Chem. Soc.* **1997**, *119*, 10382−10400. (b) Besson, C.; Finney, E. E.; Finke, R. G. *J. Am. Chem. Soc.* **2005**, *127*, 8179−8184.

(13) For a review of the kinetics and mechanisms involved in nanoparticle formation and growth, see: (a) Mondloch, J. E.; Bayram, E.; Finke, R. G. *J. Mol. Catal. A* **2012**, *355*, 1−38. (b) Wang, F.; Richards, V. N.; Shields, S. P.; Buhro, W. E. *Chem. Mater.* **2014**, *26*, 5−21.

(14) Morris, A. M.; Watzky, M. A.; Agar, J. N.; Finke, R. G. *Biochemistry* **2008**, *47*, 2413−2427.

(15) Blackmond, D. G. *Angew. Chem., Int. Ed.* **2009**, *48*, 386−390.

(16) (a) Cecchi, L.; De Sarlo, F.; Machetti, F. *Tetrahedron Lett.* **2005**, *46*, 7877. (b) Cecchi, L.; De Sarlo, F.; Machetti, F. *Eur. J. Org. Chem.* **2006**, 4852. (c) Machetti, F.; Cecchi, L.; Trogu, E.; De Sarlo, F. *Eur. J. Org. Chem.* **2007**, 4352. (d) Guideri, L.; De Sarlo, F.; Machetti, F. *Chem.—Eur. J.* **2013**, *19*, 665. (e) De Sarlo, F.; Machetti, F. In *Methods and Apllications of Cycloaddition Reactions in Organic Synthesis*, 1st ed.; Nishiwaki, N., Ed.; John Wiley & Sons, Inc.: New York, 2014; pp 205−222. (f) Biagiotti, G.; Cicchi, S.; De Sarlo, F.; Machetti, F. *Eur. J. Org. Chem.* **2014**, 7906−7915. (g) Trogu, E.; Vinattieri, C.; De Sarlo, F.; Machetti, F. *Chem.—Eur. J.* **2012**, *18*, 2081.

(17) Benson, S. W. *J. Chem. Phys.* **1956**, *20*, 1605−1612.

(18) Hein, J. E.; Cao, B. H.; Viedma, C.; Kellogg, R. M.; Blackmond, D. G. *J. Am. Chem. Soc.* **2012**, *134*, 12629.

(19) (a) Spokes, G. N.; Benson, S. W. *J. Am. Chem. Soc.* **1967**, *89*, 6030. (b) Khrapkovskii, G. M.; Shamov, A. G.; Nikolaeva, E. V.; Chachkov, D. V. *Russ. Chem. Rev.* **2009**, *78*, 903.

(20) Pascal, R.; Taillades, J.; Commeyras, A. *Tetrahedron* **1978**, *34*, 2275.

(21) Matt, C.; Wagner, A.; Mioskowski, C. *J. Org. Chem.* **1997**, *62*, 234.

(22) Clayden, J.; Greeves, N.; Warren, S.; Wothers, P. *Organic Chemistry*; Oxford University Press: Oxford, 2001; p 934.

DOI: 10.1021/ja512753v
J. Am. Chem. Soc. 2015, 137, 2386−2391